Semianalytical Solutions to the Lighthill–Whitham–Richards Equation With Time-Switched Triangular Diagrams: Application to Variable Speed Limit Traffic Control

Yang Shao[®], Michael W. Levin, Stephen D. Boyles, and Christian G. Claudel

Abstract—This article proposes a new approach for computing a semiexplicit form of the solution to a class of traffic flow problems encoded by a Hamilton-Jacobi (HJ) partial differential equation (PDE), with time-switched Hamiltonian. Using a characterization of the problem derived from viability theory, we show that the solution associated with the problem can be formulated as a minimization problem involving the trajectory of an auxiliary dynamical system. A generalized Lax-Hopf formula for the switched Hamiltonian problem is derived, which enables us to compute the solution associated with affine initial or boundary conditions as a linear program involving the control function of the auxiliary dynamical system. This formulation allows us to compute the solution to the original problem exactly, unlike dynamic programming methods. In addition, this method allows one to very efficiently recompute the boundary conditions associated with an initial condition problem, allowing large-scale variable speed limit traffic control problems to be solved.

Note to Practitioners—Most dynamic speed limit control techniques used to manage traffic flow on highways rely on discretizations of partial differential equations, which require one to compute the solution on a computational grid. This article focuses on an alternate solution method that does not require the solution to be found on all grid points, potentially saving computational time on large-scale problems.

Index Terms—Linear programming, speed control, switched fundamental diagrams.

Manuscript received October 2, 2020; accepted November 12, 2020. This article was recommended for publication by Associate Editor S. Dadras and Editor Q. Zhao upon evaluation of the reviewers' comments. This work was supported by the Center for Advanced Multimodal Mobility Solutions and Education (CAMMSE) and the National Science Foundation under Grant 1636154 and Grant 1739964. (Corresponding author: Christian G. Claudel.)

Yang Shao is with the School of Modern Posts (Logistics School), Xi'an University of Posts and Telecommunications, Xi'an 710061, China, also with the Institute of Posts, Xi'an University of Posts and Telecommunications, Xi'an 710061, China, and also with the Department of Civil, Architectural and Environmental Engineering, The University of Texas at Austin, Austin, TX 78712-0273 USA (e-mail: shaoyang2020@xupt.edu.cn).

Michael W. Levin is with the Department of Civil, Environmental, and Geo-Engineering, University of Minnesota, Minneapolis, MN 55455 USA (e-mail: mlevin@umn.edu).

Stephen D. Boyles and Christian G. Claudel are with the Department of Civil, Architectural and Environmental Engineering, The University of Texas at Austin, Austin, TX 78712-0273 USA (e-mail: sboyles@mail.utexas.edu; christian.claudel@utexas.edu).

Color versions of one or more figures in this article are available at https://doi.org/10.1109/TASE.2020.3039836.

Digital Object Identifier 10.1109/TASE.2020.3039836

I. INTRODUCTION

A. Background and Motivation

NTELLIGENT transportation systems have proposed a variety of traffic control devices that induce time-dependent traffic behaviors to reduce congestion. Examples include variable speed limits (see [1]–[12]) and dynamic lanes reversal (see [13], [14]). Several of these devices have the common effect of causing different flow–density relationships at different time intervals on a section of road. For instance, variable speed limits change the shape of the uncongested region (see [15], [16]) due to the different free-flow speeds.

Of the three levels of traffic flow models (macroscopic, mesoscopic, and microscopic), macroscopic models offer tractability for studying larger networks while including time-varying changes in flow caused by these control devices. Macroscopic models are typically based on the Lighthill-Whitham-Richards (LWR) partial differential equations (PDEs) of traffic flow [17], [18]. There are several well-known approximation methods for solving the LWR PDE, such as the cell transmission model (CTM) [19], [20] and the link transmission model [21]. Although effective for dynamic network loading, these approximations nevertheless contain numerical errors and/or limitations that motivate finding an exact solution. For instance, cell lengths in the CTM are determined by free-flow speeds, which causes numerical errors in the propagation of waves (both in free flow and congestion) as well as reducing its suitability for modeling variable speed limit situations. In contrast, the LTM (as the algorithm introduced in this article) does not exhibit such limitations. The LTM is a very powerful solution method that has been widely used in network loading applications [22]. While extremely efficient computationally, the LTM is usually restricted to situations in which initial conditions are increasing over space (no expansion waves), while this article considers general initial conditions.

B. Problem Statement

The LWR PDE with a fixed, triangular flow-density relationship has been solved exactly using a Lax-Hopf method [23], [24]. The main difference between this article and [23] is the hybrid model used. Claudel and Bayen [23]

1545-5955 © 2020 IEEE. Personal use is permitted, but republication/redistribution requires IEEE permission. See https://www.ieee.org/publications/rights/index.html for more information.

considered hybrid solution components, corresponding to the solutions of the LWR model with constant (in space and time) model parameters, but associated with target functions defined on a set of nonempty interior. While these target functions can describe another dynamic on their domain of definition (for example, an LWR model with different model parameters or a model that is not LWR), they have to be prescribed in advance and are cumbersome to use. In the present case, we consider classical initial and boundary condition functions (with empty interior) and consider instead switched model parameters.

The contributions of this article are to extend the Lax-Hopf method to a triangular switched (in time) flow-density relationship (the Hamiltonian when writing the LWR model as its equivalent Hamilton-Jacobi (HJ) PDE). The switched flow-density relationship may take a different form at different time intervals. Specifically, we solve the following mathematical problem.

Given an HJ PDE with switched (in time) triangular Hamiltonian, given an initial condition, and given upstream and downstream boundary conditions, how can the solution to this equation at any point in space and time be exactly and efficiently computed in a single step?

Control theory (and in particular viability theory) provides the appropriate tools (an exclusively constructed semianalytical solution by using a Lax-Hopf formula) to solve this problem.

For any single boundary condition (initial, upstream, or downstream), the solution to the HJ equation [25]–[27] with switched Hamiltonians is found through a linear program. The solution for a set of initial boundary conditions is the minimum of the solutions to a set of linear programs that exhibit similar constraint structure and may be solved in parallel. After developing the solution method, we explore the characteristics of solutions and application to variable speed limits.

The rest of this article is organized as follows. Sections II and III provide background information on the LWR model and viability episolutions to this model, respectively. Section IV provides a generalized Lax–Hopf formula associated with our model, and Section V shows how the case of affine initial and boundary conditions can be handled with linear programming. Section VI discusses the generalization to piecewise affine initial and boundary conditions. Section VII discusses solution validity, and Section VIII shows how the model and solution method developed in this article can be applied to variable speed limit control. Finally, Section IX concludes this article.

II. BACKGROUND

A. Lighthill-Whitham-Richards Traffic Flow Model

For the remainder of the article, we will assume that the spatial domain representing the highway section is $[x^{\flat}, x^{\sharp}]$, where x^{\flat} and x^{\sharp} , respectively, represent the upstream and downstream boundaries of the domain. Traffic flow on this section can be described by the density function, denoted as $\rho(\cdot, \cdot)$. The density function represents an aggregated number of vehicles per space unit and can be modeled by the LWR

PDE

$$\frac{\partial \rho(t,x)}{\partial t} + \frac{\partial \psi(\rho(t,x),t)}{\partial x} = 0.$$
 (1)

The function $\psi(\cdot, \cdot)$ is named the flux function, which we assume to be a function of both density and time. It depends on several empirical parameters (e.g., the maximal speed, the number of lanes, and the drivers habits). Different models have been proposed for ψ , in particular the triangular model defined next, this model that is widely used in the literature [19], [20], [28], [29]

$$\psi(\rho, t) = \begin{cases} v(t)\rho, & \text{if } \rho \le \rho_c(t) \\ w(t)(\rho_m(t) - \rho), & \text{otherwise.} \end{cases}$$
 (2)

In (2), the parameters ρ_m , ρ_c , v(t), and w(t) are all positive. We assume that the fundamental diagram is a continuous function of density, which implies the condition

$$\omega(t)\rho_m(t) = (v(t) + \omega(t))\rho_c(t). \tag{3}$$

In the remainder of this article, we assume that the flux function is triangular and given by (2). Triangular diagrams are extremely common in the transportation literature since they are robust and require only three parameters, v(t), $\rho_c(t)$, and w(t) for their calibration, which is assumed to be piecewise constant in time. v(t) is the free-flow speed, w(t) is the congested wave speed, and $\rho_c(t)$ is the critical density at which the maximum flow is achieved. $\rho_m(t)$ is the jam density and can be deduced from the other three parameters. In this article, the fundamental diagram is assumed to be switched in time, that is, the parameters v(t) and $\rho_c(t)$ are piecewise constant functions of time. These time switches can, for example, model time-varying changes of the properties of the physical domain, most often a change in the maximal velocity allowed on the domain v(t) or a change in the number of lanes of the domain [which affects $\rho_c(t)$], by closing or opening a lane to traffic. Since the LWR model is a first-order traffic flow model with instant adaptations to flow or density changes, such time switches have an instant effect on traffic, leading to somewhat unrealistic behavior (e.g., abrupt discontinuities in speed when a new free-flow speed is imposed). Such discontinuities are a feature of the LWR model and occur even if parameters are not switched in time, for example, when traffic speed jumps from zero to critical velocity instantly when clearing a traffic jam [30].

B. Hamilton-Jacobi Equation

Equivalently, the state of traffic can be described by a scalar function $\mathbf{M}(\cdot, \cdot)$ of both time and space, known as the Moskowitz function [31], [32]. The Moskowitz function is a macroscopic description of traffic flow, which appears naturally in the context of traffic. It can be interpreted as follows. Let consecutive integer labels be assigned to vehicles entering the highway at location $x = x^b$. The Moskowitz function $\mathbf{M}(\cdot, \cdot)$ is assumed to be continuous and satisfies $\lfloor \mathbf{M}(t, x) \rfloor = n$, where n is the label of the vehicle located in x at time t [20], [28].

The density function $\rho(\cdot, \cdot)$ is related [32] to the spatial derivative of the Moskowitz function $\mathbf{M}(\cdot, \cdot)$ as follows:

$$\rho(t,x) = -\frac{\partial \mathbf{M}(t,x)}{\partial x}.$$
 (4)

If the density function is to be modeled by the LWR PDE, the Moskowitz function satisfies an HJ PDE obtained [20], [23], [34] by integration of the LWR PDE

$$\frac{\partial \mathbf{M}(t,x)}{\partial t} - \psi \left(-\frac{\partial \mathbf{M}(t,x)}{\partial x}, t \right) = 0.$$
 (5)

Equation (4) can also be interpreted as the flow-density relationship $q(t, x) = \psi(\rho(t, x), t)$, where $\rho(t, x)$ is given by (3) and $q(t, x) = (\partial \mathbf{M}(t, x))/\partial t$.

In this article, we focus on the Moskowitz function rather than the density function since the Moskowitz function is continuous and is the solution to the HJ equation (4) that is easier to deal with numerically. Several classes of weak solutions to (4) exist, such as viscosity solutions [24], [35], [36] or Barron-Jensen/Frankowska (B-J/F) solutions [28], [37]. For the problem investigated in this article, these solutions are equivalent and can be computed implicitly using a Lax-Hopf formula. The equivalence arises from the fact that the initial and boundary conditions are continuous functions (with no internal conditions) and that no lower viability constraints are present (unlike in [38] for instance). In this situation, the viability episolution to (4), which is only lower semicontinuous in general, becomes continuous, and the representation formulas of the solution, which can be found in [21], [24], and [28], are all identical.

The fact that the solution is continuous (instead of only lower semicontinuous) is also very important since the experimental cumulative number of vehicles function [see (4)] is continuous [21].

C. B-J/F Solutions to HJ Equations

In order to characterize the B-J/F solutions, we first need to define the convex transform of the Hamiltonian $\psi(\cdot, \cdot)$ as follows.

Definition 1 (Convex Transform): For an upper semicontinuous (with respect to its first argument) Hamiltonian $\psi(\cdot, \cdot)$, the convex transform $\varphi^*(\cdot, \cdot)$ is given by

$$\varphi^*(u,t) := \sup_{p \in \text{Dom}(\psi(\cdot,t))} [p \cdot u + \psi(p,t)]. \tag{6}$$

In the present case, the convex transform $\phi^*(u,t)$ is given by a switched triangular Hamiltonian $\phi^*(u,t) = (u+v) * \rho_c$, and the convex transform $\phi^*(u,t)$ is a piecewise linear function of u, with time-varying (switched) coefficients. Note that the definition of the convex transform is derived from the Legendre–Fenchel transform modulo a sign change and was introduced in [33]. The pseudocontrol u corresponds to the optimization variable in the Lax–Hopf formula, which continuously varies between -v and +w (represented here as $[v^{\text{flat}}, v^{\sharp}]$). When solving the optimal control problem, the value that the pseudocontrol takes is usually the forward or backward wave speed (-v) or w due to our negative sign convention), though not always, for example, when calculating the solution in an expansion wave (fan).

Solving the HJ PDE (5) requires the definition of value conditions, which encode the traditional concepts of initial, boundary, and internal conditions.

Definition 2 (Value Condition): A value condition $\bar{c}(t, x)$ is a lower semicontinuous function defined on a subset of $[0, t_{\text{max}}] \times [x^{\flat}, x^{\sharp}]$.

For formulation purposes, it is convenient to refer to a value condition outside of its domain. We expand the value condition by defining the extended value condition $\mathbf{c}(\cdot, \cdot)$ as follows:

$$\vec{c}(t,x) = \begin{cases} \vec{c}(t,x), & \text{if } (t,x) \in \text{Dom}(\vec{c}) \\ +\infty, & \text{elsewhere.} \end{cases}$$
 (7)

A value condition can encode any constraint on the value of the Moskowitz function that we need to encode, for instance, a constraint on its value at the initial time (also known as an initial condition), a constraint of its values at the upstream or downstream boundaries of the domain (called upstream and downstream boundary conditions), or a constraint of its value inside the computational domain (internal condition, which corresponds to a fixed or moving bottleneck for practical purposes, though other types of conditions are possible such as hybrid conditions [39]).

III. VIABILITY EPISOLUTIONS

In the present context, we recall a specific control framework based on viability theory [33], [40], [41]. This control framework is identical to the framework developed in [33]. We then extend this framework to piecewise constant (switched) triangular diagrams, which was not investigated in [33]. We first recall a definition from viability theory [33], [40], [41], which we later use in the article.

Definition 3 ([40], [41] Capture Basin): Given a dynamical system F and two sets K (called the constraint set) and C (called the target set) satisfying $C \subset K$, the capture basin $\operatorname{Capt}_F(K, C)$ is the subset of states of K from which there exists at least one evolution solution of F reaching the target C in finite time while remaining in K.

Definition 3 will be used throughout this article. Note that there are several ways to compute the capture basin $\operatorname{Capt}_F(\mathcal{K}, \mathcal{C})$ numerically, in particular using the capture basin algorithm [42], [43]. We now introduce the auxiliary dynamical system used to compute B-J/F solutions to the HJ PDE (5).

Definition 4 (Auxiliary Dynamical System): Given a Hamiltonian $\psi(\cdot)$ with convex transform $\varphi^*(\cdot)$, we define an auxiliary dynamical system F associated with the HJ PDE (5)

$$F_T := \begin{cases} \tau'(t) = -1 \\ x' = u(t) \\ y' = -\varphi^*(u(t), T - t) \end{cases}$$
(8)

where $u(t) \in \text{Dom}(\varphi^*(\cdot, T - t))$ is called auxiliary control of the dynamical system F_T .

The controls $u(\cdot)$ associated with the dynamical system are integrable functions with values in $\bigcup_{t \in [0,T]} \text{Dom}(\varphi^*(\cdot, T-t)) \times \{T-t\}$ (they can be noncontinuous). Furthermore, the above system of differential equations is valid for all $t \geq 0$ except possibly for a set of zero measure. We now introduce specific expressions for the viability domain \mathcal{K} and the target set \mathcal{C} ,

which play a role in the definition of the proper capture basin used to define the solution to the HJ PDE.

Definition 5 (Constraint Set Associated With an HJ PDE): For an HJ PDE (5) defined in the set $\mathbb{R}_+ \times [x^{\flat}, x^{\sharp}]$, we define the constraint set \mathcal{K} as $\mathcal{K} := \mathbb{R}_+ \times [x^{\flat}, x^{\sharp}] \times \mathbb{R}$.

We refer the reader to [33] for the construction of solutions associated with general epigraphical environment sets (where $\mathcal K$ is the epigraph of a given lower constraint function), and the mathematical interpretation of the resulting solutions. The target set encodes boundary measurement data as follows.

Definition 6 (Target Set Associated With an HJ PDE): For an HJ PDE (5) defined in $\mathbb{R}_+ \times [x^{\flat}, x^{\sharp}]$, we define a target function as a lower semicontinuous function $\mathbf{c}(\cdot, \cdot)$ in a subset of $\mathbb{R}_+ \times [x^{\flat}, x^{\sharp}]$. The target function \mathbf{c} defines an epigraphical target set as $\mathcal{C} := \mathcal{E}\mathrm{pi}(\mathbf{c})$. This set is the subset of triples $(t, x, y) \in \mathbb{R}_+ \times [x^{\flat}, x^{\sharp}] \times \mathbb{R}$ such that $y \geq \mathbf{c}(t, x)$ (it is the epigraph of the function \mathbf{c}).

Definition 1 of the capture basin can now be applied to the specific target C given by Definition 6 in the constraint set K given by Definition 5 with the dynamics (8).

Definition 7 (Viability Episolution): Given a characteristic system F., a constraint set \mathcal{K} , and a target set \mathcal{C} , respectively, defined by Definitions 4–6, the viability episolution \mathbf{M} is defined by

$$\mathbf{M}(t,x) := \inf_{(t,x,y) \in \text{Capt}_{E_t}(\mathcal{K},\mathcal{C})} y. \tag{9}$$

Note that by definition, the capture basin $\operatorname{Capt}_F(\mathcal{K}, \mathcal{C})$ of a target \mathcal{C} viable in the environment \mathcal{K} is the subset of initial states (t, x, y), for which there exists a measurable control $u(\cdot)$ such that its associated evolution

$$s \mapsto \left(t - s, x + \int_0^s u(\tau)d\tau, y - \int_0^s \varphi^*(u(\tau), t - \tau)d\tau\right) \quad (10)$$

is viable in \mathcal{K} until it reaches the target \mathcal{C} . Here, τ is a pseudo time that runs backwards in time, whereas t is fixed. It is called "episolution" of the HJ PDE (5) because it is defined by its epigraph, i.e., by (9), which states that the graph of $\mathbf{M}(\cdot, \cdot)$ is the lower envelope of the capture basin $\operatorname{Capt}_F(\mathcal{K}, \mathcal{C})$. The viability episolution \mathbf{M} defined by (9) is shown in [33] to be a B-J/F solution to (5). If furthermore \mathbf{M} is differentiable, then it is a classical solution to (5).

IV. GENERALIZED LAX-HOPF FORMULA

A. Semiexplicit Expression of the Viability Episolution

In this section, we use this concept of viability episolution to construct a semiexplicit Lax-Hopf formula associated with this solution. This Lax-Hopf formula characterizes the solution to the HJ PDE (5), for any type of time-varying Hamiltonian. In Sections V and VI, we will derive the simplified formula allowing the computation of solutions to (5), for arbitrary switched (in time) triangular Hamiltonians.

Theorem 1 (Generalized Lax-Hopf Formula): The viability episolution $\mathbf{M_c}$ associated with a target $\mathcal{C} := \mathcal{E}\mathrm{pi}(\mathbf{c})$, for a given lower semicontinuous function \mathbf{c} , and defined by (9)

can be expressed as

$$M_c(t,x) = \inf_{(u(\cdot),T)\in R} \left[c\left(t - T, x + \int_0^T u(\tau)d\tau\right) + \int_0^T \varphi * (u(\tau), t - \tau)d\tau \right]$$
(11)

for some set R. Since $\vec{c}(t,x)$ is generally defined, it may represent both initial and boundary conditions.

Proof: It appears in the Appendix.

Although y does not play a direct role in the quantity to be minimized, it indirectly intervenes in fact that the evolution has to be viable in K until it reaches the target C. The viability in K constraints $(t - s, x + \int_0^s u(\tau)d\tau)$ to be in the space-time domain, whereas the constraint of reaching a target C imposes a lower bound on the value of y, since the epigraph corresponding to the target C has a lower boundary (corresponding to the graph of \vec{c}).

B. Semiexplicit Representation for Switched (in Time) Hamiltonians

We now assume that the Hamiltonians (fundamental diagrams) are switched in time, which is of the form $\psi(p,t) = \psi_i(p)$ for $t \in (t_{i-1}, t_i]$, where t_0, \ldots, t_n are given. The Hamiltonians have the corresponding convex transforms $\varphi_i^*(u)$.

1) Switched Lax-Hopf Formula: We first define the generalized Lax-Hopf formula for an initial condition c(0,x) valid on $x \in [0,x^{\sharp}]$ (elsewhere, $c(t,x) = \infty$). According to the Lax-Hopf formula, the density ρ_A is conserved across the switching boundary. Indeed, the solution resulting from the Lax-Hopf formula is continuous (due to the dynamical model used to generate the Lax-Hopf formula) outside of the domain of the target set, which is located at the boundaries of the computational domain $(t,x) \in (\{0\} \times [x_{\min},x_{\max}]) \cup (\mathbb{R}_+ \times \{x_{\min},x_{\max}\})$.

For simplicity, let us first consider the case in which the Hamiltonian has a single switch in time

$$\psi(p,t) = \begin{cases} \psi_1(p), & \text{if } t < \hat{t}_1 \\ \psi_2(p), & \text{if } t \ge \hat{t}_1 \end{cases}$$
 (12)

where $\psi_1(\cdot)$ and $\psi_2(\cdot)$ are concave functions, associated with the convex transforms $\varphi_1^*(\cdot)$ and $\varphi_2^*(\cdot)$.

Proposition 1: Let the initial condition c(0, x) be defined for all x. Then

$$\mathbf{M_{c}}(t,x) = \inf_{(u_{1},u_{2},T_{2})\in[v^{\flat},v^{\sharp}]^{2}\times[-\hat{t}_{1},t-\hat{t}_{1}]} c(t-T_{2}-t_{1},x+t_{1}u_{1}+T_{2}u_{2}) + \hat{t}_{1}\varphi_{1}^{*}(u_{1}) + T_{2}\varphi_{2}^{*}(u_{2}).$$
(13)

Proof (Trivial for t < \hat{t}_1): Consider $t \ge \hat{t}_1$. By definition

$$\mathbf{M_{c}}(t,x) = \inf_{(u(\cdot),T)\in[v^{\flat},v^{\sharp}]\times[0,t]} c\left(t-T,x+\int_{0}^{T} u(s)ds\right) + \int_{0}^{T} \varphi^{*}(u(s))ds \quad (14)$$

where $\varphi^*(\cdot)$ is piecewise defined by $\varphi_i^*(u)$, $i \in 1, 2$. For $T \ge \hat{t}_1$

$$\int_0^T \varphi^*(u(s))ds = \int_0^{\hat{t}_1} \varphi_1^*(u(s))ds + \int_{\hat{t}_1}^T \varphi_2^*(u(s))ds. \quad (15)$$

By Jensen's inequality

$$\int_{0}^{\hat{t}_{1}} \varphi_{1}^{*}(u(s))ds + \int_{\hat{t}_{1}}^{T} \varphi_{2}^{*}(u(s))ds$$

$$\geq \hat{t}_{1}\varphi_{1}^{*}\left(\frac{\int_{0}^{\hat{t}_{1}} u(s)ds}{\hat{t}_{1}}\right) + \left(T - \hat{t}_{1}\right)\varphi_{2}^{*}\left(\frac{\int_{\hat{t}_{1}}^{T} u(s)ds}{T - \hat{t}_{1}}\right). \quad (16)$$

Set $u_1 = (\int_0^{\hat{t}_1} u(s)ds)/\hat{t}_1$ and $u_2 = (\int_{\hat{t}_1}^T u(s)ds)/(T - \hat{t}_1)$. Then

$$\hat{t}_1 u_1 + (T - \hat{t}_1) u_2 = \int_0^{\hat{t}_1} u(s) ds + \int_{\hat{t}_1}^T u(s) ds$$
$$= \int_0^T u(s) ds. \tag{17}$$

Then

$$\mathbf{M_{c}}(t,x) = \inf_{(u_{1},u_{2},T)\in\left[v^{\flat},v^{\sharp}\right]^{2}\times\left[0,t\right]} c\left(t-T,x+\hat{t}_{1}u_{1}+\left(T-\hat{t}_{1}\right)u_{2}\right) + \hat{t}_{1}\varphi_{1}^{*}(u_{1}) + \left(T-\hat{t}_{1}\right)\varphi_{2}^{*}(u_{2}).$$
(18)

Let $T_2 = T - \hat{t}_1$. Since $T \in [0, t], T_2 \in [\hat{t}_1, t - \hat{t}_1]$. Then

$$\mathbf{M_{c}}(t,x) = \inf_{\substack{(u_{1},u_{2},T_{2}) \in [v^{\flat},v^{\sharp}]^{2} \times [\hat{t}_{1},t-\hat{t}_{1}] \\ + \hat{t}_{1}\varphi_{1}^{*}(u_{1}) + T_{2}\varphi_{2}^{*}(u_{2}).}} c(t - \hat{t}_{1} - T_{2},x + \hat{t}_{1}u_{1} + T_{2}u_{2})$$

$$(19)$$

Corollary 1: For $t > \hat{t}_1$, for all x, let $c(\hat{t}_1, x) = \mathbf{M_c}(\hat{t}_1, x)$. Then

$$\mathbf{M_{c}}(t,x) = \inf_{(u_{2},T)\in\left[v^{\flat},v^{\sharp}\right]\times\left[0,t-\hat{t}_{1}\right]} c(t-T,x+Tu_{2}) + T\varphi_{2}^{*}(u_{2}).$$
(20)

Using Corollary 1, we can generalize Proposition 1 to n time intervals. Let $\vec{u} = (u_1, \dots, u_n)$ and $\vec{\hat{t}}(T) = (\hat{t}_1 - \hat{t}_0, \dots, \hat{t}_{n-2} - \hat{t}_{n-2}, T - \hat{t}_{n-1})$. Let $\varphi^*(\vec{u}) = (\varphi_1^*(u_1), \dots, \varphi_n^*(u_n))$.

Proposition 2: Consider *n* time intervals of controls. Then, for $t > t_n$

$$\mathbf{M_{c}}(t,x) = \inf_{(\vec{u},T) \in \left[v^{\flat}, v^{\sharp}\right]^{n} \times [0,t]} c\left(t - T, x + \hat{\vec{t}}(T) \cdot \vec{u}\right) + \hat{\vec{t}}(T) \cdot \boldsymbol{\varphi}^{*}(\vec{u}). \quad (21)$$

Proof: By induction on Corollary 1.

V. STRUCTURE OF THE SOLUTIONS ASSOCIATED WITH AFFINE INITIAL, UPSTREAM, AND DOWNSTREAM BOUNDARY CONDITIONS

We now develop a system of mathematical programs to solve the switched Lax-Hopf formula given affine initial, upstream, and downstream boundary conditions. These mathematical programs are linear if $\varphi_i^*(u)$ is a linear function of u so that the term $\hat{t}(t) \cdot \varphi^*(\vec{u})$ is linear. This is satisfied if the fundamental diagram for each switch is triangular. Therefore, we assume in this section that the fundamental diagram is triangular. Triangular fundamental diagrams are used in several well-known solution methods for the kinematic wave theory [21], [44].

In order to show the significant improvement of our method, we compared the LP method in this article and the popular

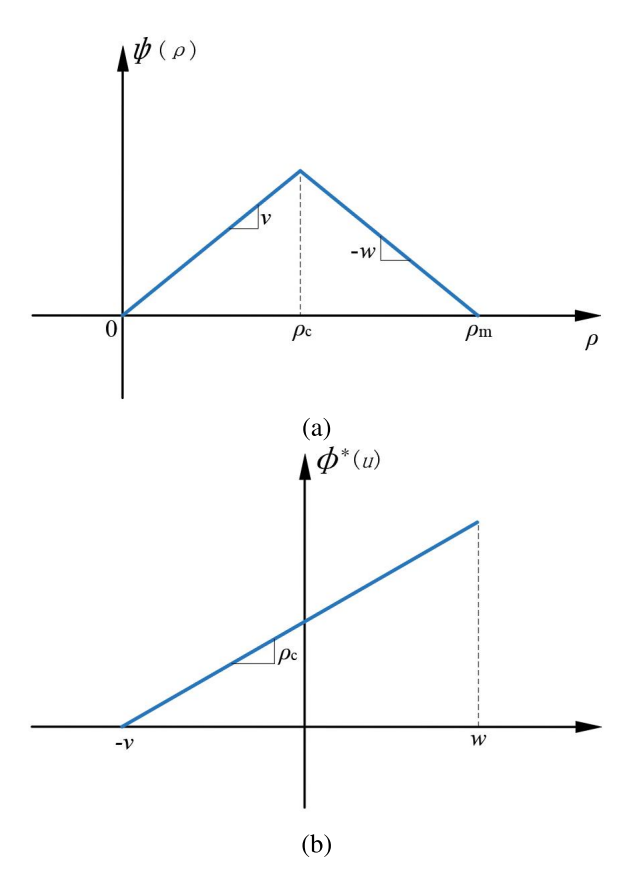


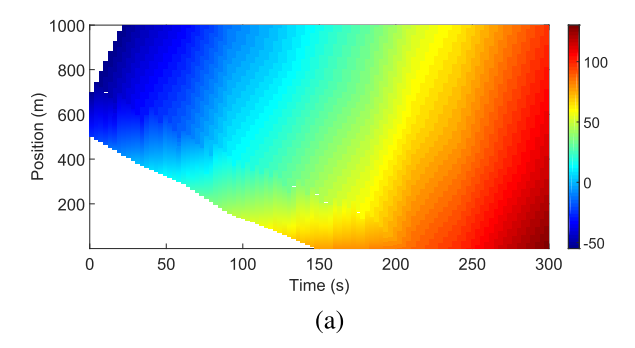
Fig. 1. (a) Triangular fundamental diagram, described by three independent parameters v, w, and ρ_m . (b) Associated convex transform.

CTM. The upstream and downstream boundary conditions are analogous to the demand and supply of CTM. While the algorithm requires the iterative construction of the boundary conditions, CTM requires the computation of the solution inside the computational domain too, which increases the computational time [22]. Unlike the CTM, the LTM does not require discretization in space and is not constrained by the CFL condition. It is a very efficient numerical scheme that has a wide variety of applications; however, its main limitation is in the integration of initial conditions. Since we want to encode general initial conditions in this article, we focus on an alternate method that we now outline.

For triangular fundamental diagrams, $\varphi_i^*(u)$ is linear

$$\varphi^*(u) = (v(\hat{t}_i) + u)\rho_c(\hat{t}_i).$$

If $\varphi_i^*(u)$ is not linear, the mathematical programs will still have linear constraints but will have general convex objectives (not necessarily linear) and will thus not be linear programs. The pseudocontrol u corresponds to the optimization variable in the Lax–Hopf formula, which continuously varies between -v and +w (represented here as $[v^{\text{flat}}, v^{\sharp}]$). When solving the optimal control problem, the value that the pseudocontrol takes is usually the forward or backward wave speed (-v) or w due to our negative sign convention), though not always, for example, when calculating the solution in an expansion wave (fan) in Fig. 1.



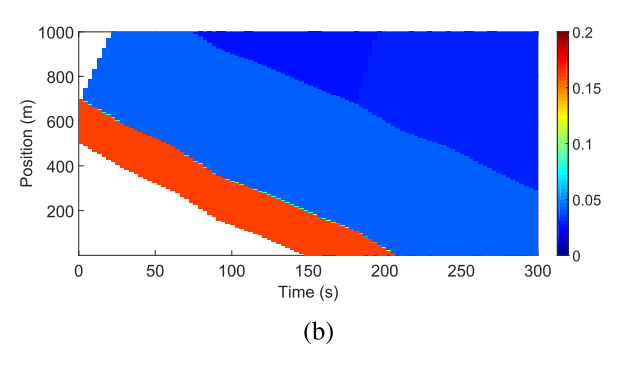


Fig. 2. Illustration of the solution associated with a single initial condition block. (a) Colormap representation of the Moskowitz function associated with a given affine initial condition block and (b) its corresponding density.

A. Affine Initial Condition

The switched Lax-Hopf formula yields the following linear program to solve $\mathbf{M}_{\mathbf{c}_b}(t,x)$ with n control intervals with a linear initial condition \mathbf{c}_b . This initial condition defines $\mathbf{c}_b(0,x)$ for $x \in [x_b^{\flat},x_b^{\sharp}]$. (Note that $[x_b^{\flat},x_b^{\sharp}]$ is the range of a boundary condition, whereas [0,L] is the spatial range of the entire link.) Let b be defined on $\{0\} \times [x_b^{\flat},x_b^{\sharp}]$. Then, the capture time T satisfies T=t since $\mathbf{c}_b(t-T,x)=\infty$ for T< t. The linear program is

$$\min \ c\left(0, x + \hat{t}(t) \cdot \vec{u}\right) + \hat{t}(t) \cdot \varphi^*(\vec{u}) \tag{22}$$

s.t.
$$v^{\flat} \le u_i \le v^{\sharp} \quad \forall 1 \le i \le n$$
 (23)

$$0_b \le x + \hat{t}(t) \cdot \vec{u} \le x_b^{\sharp}. \tag{24}$$

This linear program must be solved for each initial condition. To reduce computation time, these linear programs could be solved in parallel or the similar structure of the polyhedrons may be exploited.

We illustrate the computation of the solution associated with a linear initial condition in Fig. 2.

B. Affine Upstream Boundary Condition

For upstream boundary conditions, assume without loss of generality that each upstream boundary condition b is linear and defined between some t_b^{\flat} and t_b^{\sharp} such that there exists an s with $\hat{t}_s \leq t_b^{\flat} \leq t_b^{\sharp} \leq \hat{t}_{s+1}$. This is not limiting as upstream boundary conditions are given as piecewise linear functions in general and thus can be separated as linear blocks per the inf-morphism property. Only values $(t,x) \in [t_b^{\flat}, t_b^{\sharp}] \times \{0\}$ are defined for the upstream boundary condition. Elsewhere,

 $c(t,x)=\infty$ for x>0 or $t\notin [t_b^{\flat},t_b^{\sharp}]$. This results in decision variables u_1 through u_{s-1} unused. Therefore, define $\vec{u}_{s,n}=(u_s,\ldots,u_n)$ and $\vec{t}_{s,n}(T)=(t-T,\hat{t}_{s+1}-\hat{t}_s,\ldots,\hat{t}_{n-1}-\hat{t}_{n-2},t-\hat{t}_{n-1})$ for $s\geq 1$. However, taking the product $\hat{t}_{s,n}(T)\cdot\vec{u}_{s,n}$ as currently defined will result in the product of two decision variables in the first term (because T is also a decision variable). To address this, we prove that T and u_s are fixed under the assumption that c(t,0) is nondecreasing in t on its domain. Since c(t,0) is a cumulative count, this assumption holds for any well-defined boundary condition for the kinematic wave theory. Let

$$x_s = x + u_n(t - \hat{t}_{n-1}) + \sum_{i=s}^{n-1} u_i(\hat{t}_{i+1} - \hat{t}_i)$$
 (25)

which is the x coordinate at the intersection of the path with \hat{t}_s . In addition, it is necessary that the x coordinate of the wave path remains within the link. Therefore

$$0 \le \left(t - \hat{t}_{n-1}\right) u_n \le L \tag{26}$$

and

$$0 \le (t - \hat{t}_{n-1})u_n + \sum_{j=i}^{n-1} (\hat{t}_j - \hat{t}_{j-1})u_i \le L$$

$$\forall s + 1 < i < n - 1. \quad (27)$$

Proposition 3: Suppose that c(t,0) is nondecreasing on $(t,x) \in [t_b^{\flat}, t_b^{\sharp}] \times \{0\}$ and ∞ elsewhere. Then, $u_s = \max[v^{\flat}, x_s/(\hat{t}_s - t^{\flat})]$ and $T = t - \hat{t}_s + (x_s/u_s)$.

Proof: This follows from the nondecreasing property of c(t,x). Assume that $v^{\flat}(\hat{t}_s - t^{\sharp}) \leq x_s \leq v^{\sharp}(\hat{t}_s - t^{\flat})$. If not, there is no $u \in [0,v^{\sharp}]$ that will result in a $(t-T,x) \in [t_b^{\flat},t_b^{\sharp}] \times \{0\}$ that also satisfies $u_s = x_s/(\hat{t}_s - (t-T))$ and, therefore, will result in $c(t-T,0) = \infty$.

From Proposition 2, solving the Lax-Hopf formula for upstream boundary condition c(t-T,0) involves finding the t-T that minimizes c(t-T,0). Because c(t-T,0) is nondecreasing, the optimal t-T is the smallest $t-T \in [t^{\flat}, t^{\sharp}]$ that also satisfies $u_s \in [v^{\flat}, v^{\sharp}]$. Since $u_s = x_s/(\hat{t}_s - (t-T))$ by definition, the minimum t-T is either t^{\flat} if $x_s/(\hat{t}_s-t^{\flat}) \ge v^{\flat}$ or $t-T=\hat{t}_s-(x_s/u_s)$.

This results in the following linear program for the upstream boundary condition b:

$$\min c\left(t - T, x + \vec{t}_{s,n}(T) \cdot \vec{u}_{s,n}\right) + \vec{t}_{s,n}(T) \cdot \boldsymbol{\varphi}^*\left(\vec{u}_{s,n}\right)$$
 (28)

s.t.
$$v^{\flat} \le u_i \le v^{\sharp} \quad \forall 1 \le i \le n$$
 (29)

$$t_h^{\flat} \le \mathsf{t-T} \le t_h^{\sharp} \tag{30}$$

$$x + \vec{t}_{s,n}(T) \cdot \vec{u}_{s,n} = 0 \tag{31}$$

$$0 \le \left(t - \hat{t}_{n-1}\right) u_n \le L \tag{32}$$

$$0 \le (t - \hat{t}_{n-1})u_n + \sum_{j=i}^{n-1} (\hat{t}_j - \hat{t}_{j-1})u_i \le L$$

$$\forall s + 1 \le i \le n - 1. \tag{33}$$

We illustrate the computation of the solution associated with an affine upstream boundary condition in Fig. 3.

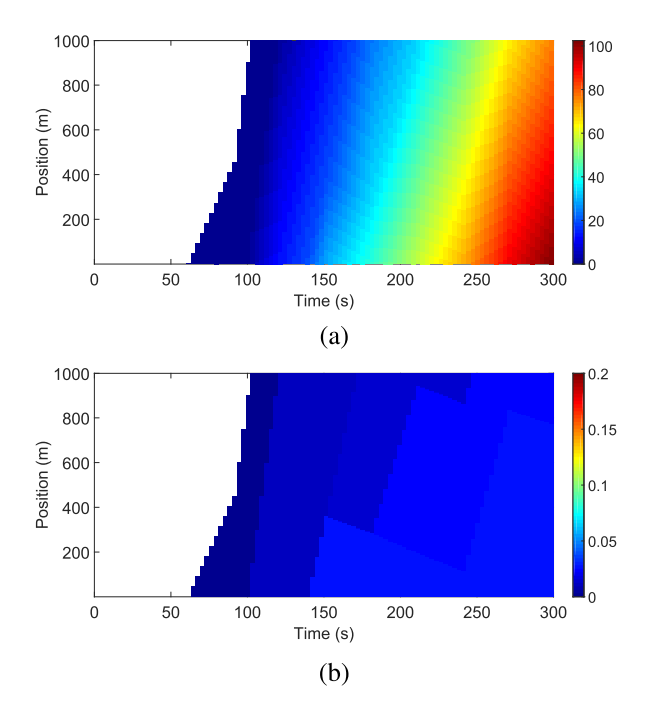


Fig. 3. Illustration of the solution associated with a single upstream boundary condition block. This figure shows a colormap representation of the Moskowitz function associated with a given linear upstream boundary condition block (a) and its corresponding density (b).

C. Affine Downstream Boundary Condition

The downstream boundary condition is similar, except that the x value corresponds to the end of the space, denoted by L. Only values $(t,x) \in [t_b^{\flat}, t_b^{\sharp}] \times \{L\}$ are defined for the downstream boundary condition. Elsewhere, $c(t, x) = \infty$. We can write an analogous statement to Proposition 3 for the downstream boundary condition.

Proposition 4: Suppose that c(t,0) is nondecreasing on $(t,x) \in [t_b^{\flat}, t_b^{\sharp}] \times \{0\}$ and ∞ elsewhere. Then, $u_s =$ $\min[v^{\flat}, (x_s - L)/(\hat{t}_s - t^{\flat})]$ and $T = t - \hat{t}_s + (x_s - L)/u_s$.

Proof: Analogous to the proof of Proposition 3.

The linear program for the downstream boundary condition b is

$$\min \ c\left(t-T,x+\vec{\hat{t}}_{s,n}(T)\cdot\vec{u}_{s,n}\right)+\vec{\hat{t}}_{s,n}(T)\cdot\boldsymbol{\varphi}^*\left(\vec{u}_{s,n}\right) \ \ (34)$$

s.t.
$$v^{\flat} \le u_i \le v^{\sharp} \quad \forall 1 \le i \le n$$
 (35)
 $t_b^{\flat} \le \text{t-T} \le t_b^{\sharp}$ (36)

$$t_b^{\flat} \le \text{t-T} \le t_b^{\sharp} \tag{36}$$

$$x + \vec{t}_{s,n}(T) \cdot \vec{u}_{s,n} = L \tag{37}$$

$$0 \le \left(t - \hat{t}_{n-1}\right) u_n \le L \tag{38}$$

$$0 \le (t - \hat{t}_{n-1})u_n + \sum_{j=i}^{n-1} (\hat{t}_j - \hat{t}_{j-1})u_i \le L$$

$$\forall s + 1 < i < n - 1. \tag{39}$$

This is identical to the linear program for an upstream boundary condition, except that $x + \hat{t}_{s,n}(T) \cdot \vec{u}_{s,n} = L$ instead of 0 since L is the downstream end.

Let \mathcal{B}^i be the set of initial conditions, \mathcal{B}^u be the set of upstream boundary conditions, and \mathcal{B}^d be the set of downstream boundary conditions, with $\mathcal{B} = \mathcal{B}^i \cup \mathcal{B}^u \cup \mathcal{B}^d$. Finding

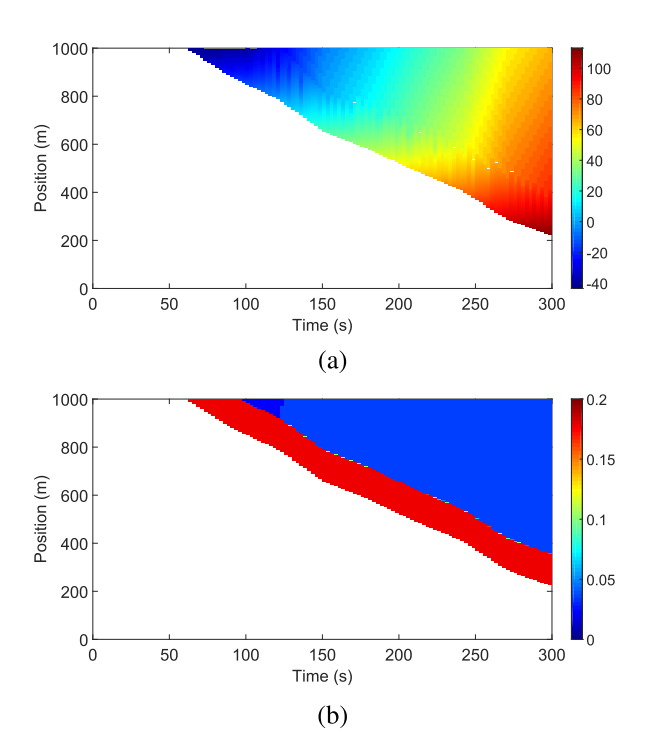


Illustration of the solution associated with a single downstream boundary condition block. (a) Colormap representation of the Moskowitz function associated with a given linear downstream boundary condition block and (b) its corresponding density.

the minimum value of $\mathbf{M}_{\mathbf{c}}(t,x)$ requires finding the minimum solution to the linear program for any boundary condition in \mathcal{B} .

We illustrate the computation of the solution associated with an affine upstream boundary condition in Fig. 4. The proposed algorithm is indeed exact but is here used to compute the solution on a rectangular grid (for visualization). The visualization software interpolates between the grid points, which causes these artifacts. Hence, the method remains grid-free but requires a grid (any grid would work, even, for example, a set of random points of the space-time domain) to visualize the function itself as a colormap. Consequently, the boundaries of the domain of definition do not appear sharp.

VI. SOLUTION TO ARBITRARY PIECEWISE AFFINE INITIAL, UPSTREAM, AND DOWNSTREAM **BOUNDARY CONDITIONS**

In general, our objective is to compute the solution associated with general piecewise affine initial, upstream, and downstream boundary conditions. This solution can be computed using the solution components associated with a single affine initial, upstream, and downstream boundary condition, introduced in Section V. The following inf-morphism property, which we now outline, states that the actual solution to the problem is the pointwise minimum of each solution component.

The inf-morphism property is crucial, in which it allows us to separate computations and focus only on computing partial solutions associated with initial and boundary blocks, which correspond to solving LPs. Without this property, the LP formulation of the solution could not be written and would instead result (in general) in a nonconvex formulation.

It is well known [40], [41] that for a given environment K, the capture basin of a finite union of targets is the union of the capture basins of these targets

$$\operatorname{Capt}_{F_T} \left(\mathcal{K}, \bigcup_{i \in I} \mathcal{C}_i \right) = \bigcup_{i \in I} \operatorname{Capt}_{F_T} (\mathcal{K}, \mathcal{C}_i) \tag{40}$$

where I is a finite set. This property essentially states that by capturing a union of targets by a dynamical system, we have to capture at least one of these targets. This property can be translated in an epigraphical form as follows.

Proposition 5 (Inf-Morphism Property): Let \mathbf{c}_i (i belongs to a finite set I) be a family of functions whose epigraphs are the targets \mathcal{C}_i . Since the epigraph of the minimum of the functions \mathbf{c}_i is the union of the epigraphs of the functions \mathbf{c}_i , and the target $\mathcal{C} := \bigcup_{i \in I} \mathcal{C}_i$ is the epigraph of the function $\mathbf{c} := \inf_{i \in I} \mathbf{c}_i$. Hence, (40) implies the following property [33]:

$$\forall t \ge 0, \ x \in \left[x^{\flat}, x^{\sharp}\right], \ \mathbf{M_c}(t, x) = \inf_{i \in I} \mathbf{M_{c_i}}(t, x). \quad (41)$$

VII. VALIDITY OF SOLUTIONS

A. Fundamental Diagrams Used for Solving HJ Equations

An important assumption, highlighted in [40], is that the Hamiltonian $\psi(\cdot)$ used in the HJ PDE (5) is not identical to the fundamental diagram $f(\cdot)$ as commonly defined. In fact, we have that

$$\psi(\rho) = \begin{cases}
v \cdot \rho, & \text{if } \rho < 0 \\
f(\rho), & \text{if } 0 \le \rho \le \rho_m \\
-w(\rho - \rho_m), & \text{if } \rho > \rho_m.
\end{cases}$$
(42)

In (42), $v = ((df(\rho))/d\rho)_{\rho=0}$ and $w = -((df(\rho))/d\rho)_{\rho=\rho_m}$. If the initial and boundary conditions are Lipschitz continuous functions that range in $[0, \rho_m]$ and $[0, q_{\text{max}}]$, respectively (where ρ_m denotes the maximal density and q_{max} denotes the capacity of the highway section), then the solution of the HJ PDE (5) is the integral of the classical LWR solution. However, if an initial density is outside of the domain $[0, \rho_m]$, it imposes a negative flow given by (42), which is nonphysical. In practice, this limits the applicability of lane-based control to situations in which the maximal density of the highway, following lane closure, is not exceeded.

B. Invalid Solutions

In the nonswitched Hamiltonian case, it was shown in [20] that the solution associated with an initial, upstream, and downstream boundary condition problem satisfies a Lipschitz property. In addition, if the initial condition is associated with densities that are in the domain of the fundamental diagram and if, furthermore, the flows associated with the upstream and downstream boundary conditions are in the image of the fundamental diagram (i.e., the flow is nonnegative and less or equal to the capacity), then the densities and flows associated with the solution are within the domain of the fundamental diagram and within the image of the fundamental diagram,

respectively. Thus, one cannot obtain unreasonable results, provided that the initial, upstream, and downstream boundary conditions are physically meaningful.

Note that being under the capacity will not guarantee that the flow will apply at a particular time step if a queue spills back (downstream boundary) or if there is insufficient demand (upstream condition). Since the proposed approach iteratively computes the flow at the boundaries, the actual flow may be less than the desired flow. A sufficient condition to ensure that the flows are nonnegative and densities are within the domain of definition of the fundamental diagram in each time zone is that the boundary flows are nonnegative and less or equal to the capacity in the corresponding time domain. This condition does not ensure that the flow condition will strictly apply, but it ensures that the solution itself does not have negative flow or density values or density values above the maximal density in the considered region.

For any type of fundamental diagram (switched or not), viability theory [33], [45] implies that at any point (t, x) of the computational domain, the optimal control $u_{\text{opt}}(t, x)$ satisfies $u_{\text{opt}}(t, x) \in \partial_+ \psi(\rho(t, x), t)$, that is, the optimal control belongs to the superdifferential of the fundamental diagram, taken at the point $\rho(t, x)$ corresponding to the density of traffic at (t, x). In particular, when the fundamental diagram is differentiable, we have that $u_{\text{opt}}(t, x) = -(\partial \psi(\rho(t, x), t))/\partial \rho$. This property is well known, in which it states that the speed of characteristics $(-u_{\text{opt}}(t, x))$ is equal to the derivative of the fundamental diagram, corresponding to the density associated with the characteristics.

In the present situation, the fundamental diagram is nondifferentiable. Since $u_{\text{opt}}(t,x) \in \text{Dom}(\varphi^*(\cdot,t))$ by construction of the problem, we can only say that the characteristics can be associated with some densities of the fundamental diagram, but nothing more. A point should be noted that the problem of switching a lane is more a limitation in applicability than a problem with model parameters.

In particular, the problem of switching a lane is more a limitation in applicability than a problem with model parameters.

If the domain of definition $[0, \rho_m]$ of the fundamental diagram is independent of time, then the densities and flows associated with all points of the solution will fall in the allowable range (respectively, $[0, \rho_m]$ and $[0, q_{\text{max}}]$). Indeed, in this situation, we can view the switched fundamental diagram forward simulation problem as a collection of forward simulation problems, with initial densities for time section i identical to the final densities of time section i-1. Since the final densities of time section i-1 belong to $[0, \rho_m]$, and by induction, all densities in all time sections belong to $[0, \rho_m]$, and by induction, all densities in all time sections belong to $[0, \rho_m]$. In the following variable speed limit control problem, we are in this situation since we only vary the speed limit parameter v, without affecting the parameter ρ_m , and therefore do not have to worry about well-posedness.

VIII. APPLICATION TO VARIABLE SPEED LIMIT CONTROL A. Problem Definition

In this section, we are interested in controlling the flow of traffic on a single highway section, using the linear

TABLE I								
PARAMETERS								

Time sections	0-30	30-60	60-90	90-120	120-150	150-180	180-210	210-240	240-270	270-300
Free flow speed (m/s)	30	25	20	40	23	35	38	27	24	32
Congestion speed (m/s)	4	3	4.5	2.5	3	2.7	4.1	2.3	3.6	3.2
Critical Density (vehicle/m)	0.2	0.2	0.2	0.2	0.2	0.2	0.2	0.2	0.2	0.2
Q	0.9									
b	8									
Demand (vehicle/s)	0.02	2.0	0.05	0.5	0.3	0.3	0.5	0.3	0.3	0.4
Supply (vehicle/s)	0.4	0.1	0.1	0.4	0.1	0.1	0.4	0.1	0.1	0.2

programming solver shown earlier. We assume that the traffic on the section of highway is modeled by the LWR model with triangular Hamiltonian. We further assume that the maximal density ρ_m and the congested velocity w are identical on the computational domain. Because of condition (3), a change in free-flow velocity thus causes a corresponding change in critical density ρ_c . The free-flow speed v(t) is assumed to be piecewise constant across the domain, with switches occurring at times t_1, \ldots, t_n , with $t_1 < t_2 < \cdots < t_n$

$$v(t) = \begin{cases} v_1, & \text{if } t \in [0, t_1] \\ v_2, & \text{if } t \in [t_1, t_2] \\ \dots \\ v_n, & \text{if } t \in [t_{n-1}, t_n]. \end{cases}$$
(43)

B. Solution Method

To solve the abovementioned problem, we choose a gradient descent approach based on the fast forward simulation scheme introduced earlier as follows. We first initialize the initial velocity guess $[v_1, \ldots, v_n]$ in $[v_{\min}, v_{\max}]^n$, where v_{\min} and v_{\max} , respectively, correspond to the minimum and the maximum free-flow velocity allowed by the controller. We consider the cost function as follows:

$$f = \sum_{i=1}^{N} (M_{\text{upstream}}(i) - M_{\text{downstream}}(i))$$
$$+ \lambda \cdot M_{\text{downstream}}(i) + K \sum_{i=1}^{n} v_{i}. \quad (44)$$

The first term corresponds to a minimization of the average accumulation of vehicles at all times, whereas the second term corresponds to a maximization of the cumulated outflow (the initial condition of the problem being fixed). The third term penalizes the use of high free-flow speeds and represents a "budget" for the traffic controller. To ensure realistic control inputs, we set a lower limit of 15 m/s and an upper limit of 45 m/s on all free-flow speeds.

Using the fast forward simulation scheme introduced earlier, we compute the cost f associated with a given vector of free-flow speed $[v_1, \ldots, v_n]$ and numerically compute the gradient g of f by perturbing each of the velocities independently. We then use a gradient descent approach, with an update equation $[v_1(k), \ldots, v_n(k)] = [v_1(k-1), \ldots, v_n(k-1)] - g\delta v$. For simplicity, we choose a constant δv as a step size. This is motivated by the fact that precision is not extremely important since vehicles do not precisely track the free-flow velocity

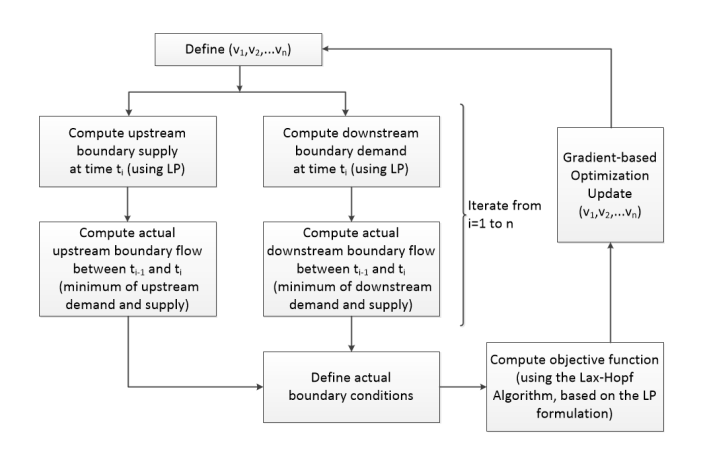


Fig. 5. Gradient-based speed control process on a highway section. The velocity optimization algorithm is based on a gradient descent approach: a set of velocities (v_1,\ldots,v_n) is first set. The LP formulation of IV is then used to compute the boundary demands and supplies and the corresponding actual boundary flows. Once these flows are computed, the same formulation is used to compute the objective function, by computing the solution on the points of the space–time domain that are relevant to the objective. A gradient-descent approach is then used to update the value of (v_1,\ldots,v_n) until the algorithm converges.

(an error of 1 m/s on each free-flow velocity is acceptable). The complete process is summarized in Fig. 5.

For this specific problem, we choose the parameters in Table I.

The results are shown in Fig. 6. Fig. 6 refers to the components of the gradient vector associated with the chosen objective function. Since the decision variable has only three elements in this application, the gradient vector has three components.

One of the greatest benefits of the proposed approach is its ability to solve the problem without having to compute the solution over an entire computational grid. By construction, the algorithm only needs to determine the actual boundary conditions of the problem (using the upstream demand and downstream supply data) and set the corresponding boundary conditions. Once this is done, the algorithm only needs to compute the solution at the points of the space–time domain required by the objective function, which can require significantly fewer operations than classical variable speed limit control methods based on the variational theory [46]–[48] or on the CTM.

C. Comparison With CTM

The CTM is a popular numerical method proposed by Daganzo [19] to solve the kinematic wave equation [17], [18].

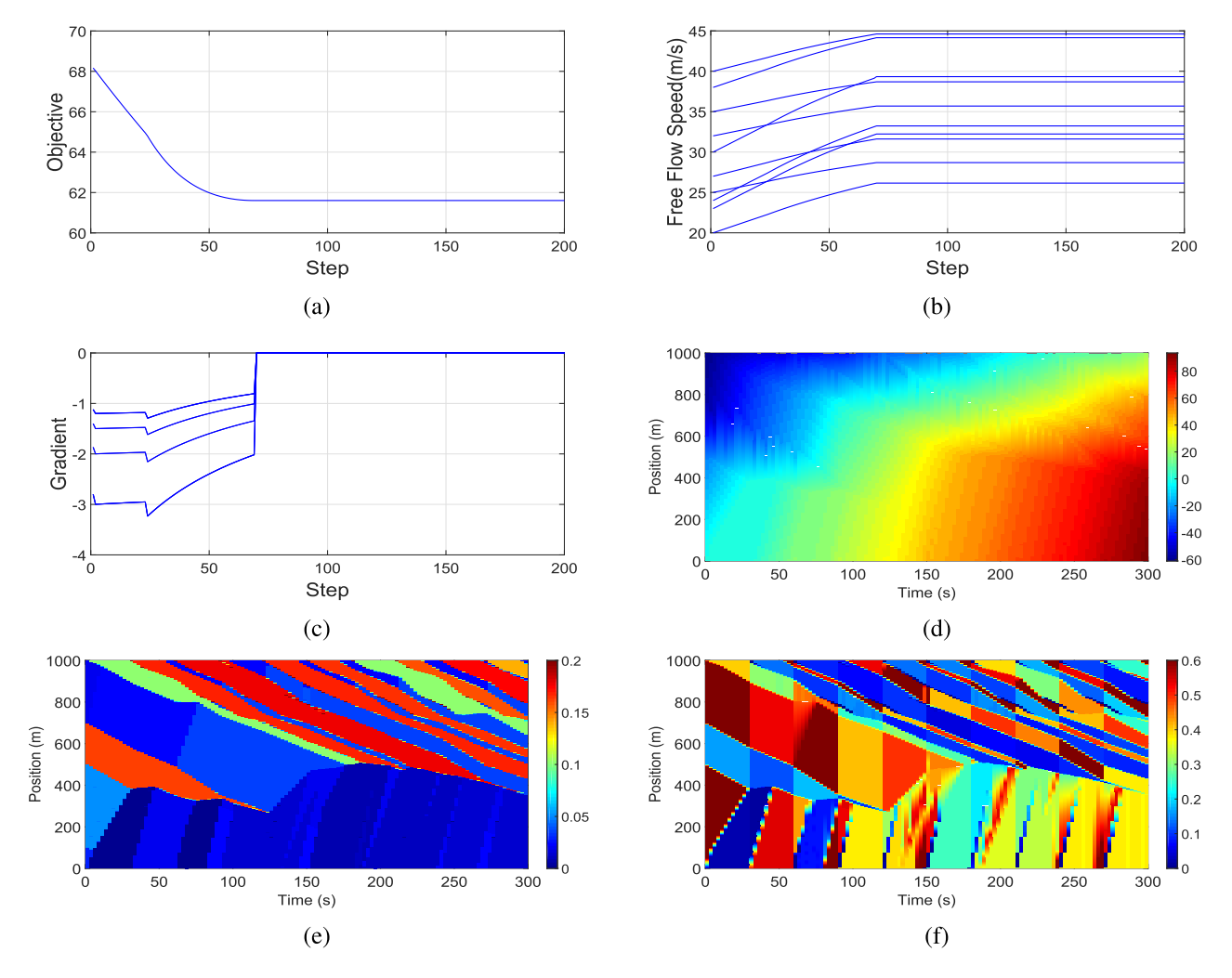


Fig. 6. Switched free-flow speed control. In this problem, we want to compute the optimal free-flow velocities to apply during three time intervals $[0, t_1]$, $[t_1, t_2]$, and $[t_2, t_3]$ to minimize the objective f defined earlier. (a) Evolution of the objective function. (b) Evolution of the free-flow speeds. (c) Gradient components. (d) Moskowitz function corresponding to the optimal free-flow velocities sequence. (e) Corresponding density associated with the Moskowitz function. (f) Flow associated with the Moskowitz function. As can be seen in this subfigure, speed limit changes can cause discontinuities in the flow.

Lebacque [49] later showed that the CTM is the first-order Godunov discretization of the LWR model [50].

The CTM predicts macroscopic traffic behavior on a given corridor by evaluating the flow and density at a finite number of intermediate points at different time steps. This is done by dividing the corridor into homogeneous sections (hereafter referred to as cells). The length of each cell is lower constrained by the time step and the free-flow speed, through the CFL condition [19], [51]. The traffic behavior is evaluated every time step starting at t = 1, 2, ..., m. The solution is evaluated at every time step for every cell. The initial and boundary conditions are required to iteratively compute the solution over each cell.

For fairness of comparison, we assume that the CTM time step is as high as possible, under the constraint that it satisfies the CFL condition. Since the maximum free-flow speed is 40 m/s and the chosen discretization of the initial condition is 100 m, the time step has to be less than 2.5 s. In CTM, the only restriction is cell size/time step > maximum free-flow speed (40 m/s in this article). The number of cells and the number of

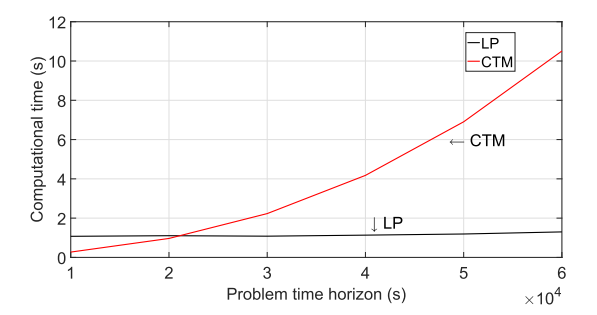


Fig. 7. Comparison of the computational time of the CTM and the Lax–Hopf approach. The horizontal axis represents the problem of time horizon and the vertical axis represents the computational time. The CTM performs better than the Lax–Hopf approach for short time horizons but is outperformed for larger horizons.

time steps have minimum multiple relationships when given a maximum free-flow speed.

Fig. 7 shows the comparison between the computational times required to optimize the free-flow speed across the

$$\begin{pmatrix}
\left(t - T, x + \int_{0}^{T} u(\tau)d\tau, y - \int_{0}^{T} \varphi^{*}(u(\tau), t - \tau)d\tau\right) \in \mathcal{E}pi(\mathbf{c}) \\
\text{and} \\
\left(t - T, x + \int_{0}^{T} u(\tau)d\tau, z - \int_{0}^{T} \varphi^{*}(u(\tau), t - \tau)d\tau\right) \in Graph(\mathbf{c})
\end{pmatrix} \Rightarrow z \leq y \tag{47}$$

highway section (given the demands of initial conditions outlined earlier), in the function of the chosen time horizon. As can be seen from Fig. 7, the computational time of the proposed approach is approximately independent of the time horizon required, whereas the CTM has an increasing computational time with the chosen time horizon. The results were obtained on a ThinkPad T470-20HD002TCD over Windows 10 Home Basic 1803, running MATLAB version R2016a. Each computational time was averaged over ten instances for reliability.

Being based on linear programs, the computational time associated with the proposed method is highly dependent on the implementation of the LP solver, and we believe that more streamlined implementations could greatly accelerate the computational time of the simulation, given that most LPs start with identical constraint matrices (but different right-hand side vectors), and thus, the overhead associated with the redefinition of each LP makes most of the observed computational time, with little time spent solving the actual LP.

IX. CONCLUSION

This article presents a formulation for solving the LWR model associated with switched (in time) triangular fundamental diagrams. We first introduce a formulation based on the viability theory, in which the problem involves the capture of targets (defined in an epigraphical form) by a time-dependent dynamical system. We show that the solution at any point in space and time can be computed by solving a linear program, which we introduce. Being semianalytical, this numerical scheme is exact. While less efficient than dynamic programming if the solution has to be computed on an entire computational grid, this method allows one to compute the solution at specific points in the domain very quickly, which is particularly useful when solving the optimization problem. This framework naturally applies to switched traffic flow control, such as dynamic speed limit control or dynamic lane control.

APPENDIX//LAX-HOPF DERIVATION

Proof of Theorem 1: We fix $(t, x) \in \mathbb{R}_+ \times [x^{\flat}, x^{\sharp}]$ and define R as the set of elements $(u(\cdot), T, y)$ belonging to $L^1(0, \infty; \text{Dom}(\varphi^*(\cdot, t)) \times \mathbb{R}_+ \times \mathbb{R}$ and satisfying viability property (45)

$$\forall s \in [0, T]$$

$$\left(t - s, x + \int_0^s u(\tau)d\tau, y - \int_0^s \varphi^*(u(\tau), t - \tau)d\tau\right) \in \mathcal{K}.$$
(45)

Equations (9) and (10) thus imply the following formula:

$$\mathbf{M_{c}}(t, x) = \inf_{(u(\cdot), T, y) \in R \text{ such that} \left(t - T, x + \int_{0}^{T} u(\tau) d\tau, y - \int_{0}^{T} \varphi^{*}(u(\tau), t - \tau) d\tau\right) \in \mathcal{E}\mathrm{pi}(\mathbf{c})} y$$

Since the graph of the target function \mathbf{c} [denoted Graph(\mathbf{c})] is the lower boundary of $\mathcal{E}\mathrm{pi}(\mathbf{c})$, we have that $z \leq y$ as shown at the top of the page.

Since Graph(c) $\subset \mathcal{E}$ pi(c), (47) and (46) imply

$$\mathbf{M}_{\mathbf{c}}(t,x) = \inf_{(u(\cdot),T,y)\in R \text{ such that}\left(t-T,x+\int_0^T u(\tau)d\tau,y-\int_0^T \varphi^*(u(\tau),t-\tau)d\tau\right)\in \text{Graph}(\mathbf{c})} y.$$

$$(48)$$

Since c is infinite outside of its domain of definition and given the definition of Graph(c), (48) can be expressed as follows:

$$\mathbf{M_{c}}(t,x) = \inf_{(u(\cdot),T,y)\in R} \left[c \left(t - T, x + \int_{o}^{T} u(\tau) d\tau \right) + \int_{o}^{T} \varphi * (u(\tau), t - \tau) d\tau \right]. \tag{49}$$

REFERENCES

- [1] G. S. van de Weg, A. Hegyi, S. P. Hoogendoorn, and B. D. Schutter, "Efficient freeway MPC by parameterization of ALINEA and a speedlimited area," *IEEE Trans. Intell. Transp. Syst.*, vol. 20, no. 1, pp. 16–29, Jan. 2019.
- [2] Y. Zhang and P. A. Ioannou, "Combined variable speed limit and lane change control for highway traffic," *IEEE Trans. Intell. Transp. Syst.*, vol. 18, no. 7, pp. 1812–1823, Jul. 2017.
- [3] G. Qian and J. B. Lee, "Variable speed limits for motorway off-ramp queue protection," *IEEE Intell. Transp. Syst. Mag.*, vol. 12, no. 2, pp. 64–76, 2020.
- [4] I. Papamichail, K. Kampitaki, M. Papageorgiou, and A. Messmer, "Integrated ramp metering and variable speed limit control of motorway traffic flow," *IFAC Proc. Volumes*, vol. 41, no. 2, pp. 14084–14089, 2008.
- [5] R. C. Carlson, I. Papamichail, M. Papageorgiou, and A. Messmer, "Optimal motorway traffic flow control involving variable speed limits and ramp metering," *Transp. Sci.*, vol. 44, no. 2, pp. 238–253, May 2010.
- [6] C. Lee, B. Hellinga, and F. Saccomanno, "Evaluation of variable speed limits to improve traffic safety," *Transp. Res. C, Emerg. Technol.*, vol. 14, no. 3, pp. 213–228, Jun. 2006.
- [7] H. Liu, L. Zhang, D. Sun, and D. Wang, "Optimize the settings of variable speed limit system to improve the performance of freeway traffic," *IEEE Trans. Intell. Transp. Syst.*, vol. 16, no. 6, pp. 3249–3257, Dec. 2015.
- [8] X. Yang, Y. Lu, and Y. Lin, "Optimal variable speed limit control system for freeway work zone operations," *J. Comput. Civil Eng.*, vol. 31, no. 1, Jan. 2017, Art. no. 04016044.
- [9] Y. Han, A. Hegyi, Y. Yuan, and S. Hoogendoorn, "Validation of an extended discrete first-order model with variable speed limits," *Transp. Res. C, Emerg. Technol.*, vol. 83, pp. 1–17, Oct. 2017.
- [10] A. Hegyi, "An overview of speed control approaches to improve freeway traffic flow," in *Proc. Eur. Control Conf. (ECC)*, Jun. 2014, pp. 2264–2267.

- [11] A. Hegyi et al., "A cooperative system based variable speed limit control algorithm against jam waves—An extension of the SPECIALIST algorithm," in Proc. 16th Int. IEEE Conf. Intell. Transp. Syst. (ITSC), Oct. 2013, pp. 973–978.
- [12] W. J. Schakel and B. van Arem, "Improving traffic flow efficiency by in-car advice on lane, speed, and headway," *IEEE Trans. Intell. Transp. Syst.*, vol. 15, no. 4, pp. 1597–1606, Aug. 2014.
- [13] M. Hausknecht, T.-C. Au, P. Stone, D. Fajardo, and T. Waller, "Dynamic lane reversal in traffic management," in *Proc. 14th Int. IEEE Conf. Intell. Transp. Syst. (ITSC)*, Oct. 2011, pp. 1929–1934.
- [14] M. W. Levin and S. D. Boyles, "A cell transmission model for dynamic lane reversal with autonomous vehicles," *Transp. Res. C, Emerg. Tech*nol., vol. 68, pp. 126–143, Jul. 2016.
- [15] M. Hajiahmadi, R. Corthout, C. Tampère, B. De Schutter, and H. Hellendoorn, "Variable speed limit control based on extended link transmission model," *Transp. Res. Rec.*, J. Transp. Res. Board, vol. 2390, no. 1, pp. 11–19, Jan. 2013.
- [16] A. Hegyi, B. DeSchutter, and J. Hellendoorn, "Optimal coordination of variable speed limits to suppress shock waves," *IEEE Trans. Intell. Transp. Syst.*, vol. 6, no. 1, pp. 102–112, Mar. 2005.
- [17] M. J. Lighthill and G. B. Whitham, "On kinematic waves. II. A theory of traffic flow on long crowded roads," *Proc. Roy. Soc. London A, Math. Phys. Sci.*, vol. 229, no. 1178, pp. 317–345, 1955.
- [18] P. I. Richards, "Shock waves on the highway," *Oper. Res.*, vol. 4, no. 1, pp. 42–51, Feb. 1956.
- [19] C. F. Daganzo, "The cell transmission model: A dynamic representation of highway traffic consistent with the hydrodynamic theory," *Transp. Res. B, Methodol.*, vol. 28, no. 4, pp. 269–287, Aug. 1994.
- [20] C. F. Daganzo, "A variational formulation of kinematic waves: Basic theory and complex boundary conditions," *Transp. Res. B, Methodol.*, vol. 39, no. 2, pp. 187–196, Feb. 2005.
- [21] I. Yperman, S. Logghe, and B. Immers, "The link transmission model: An efficient implementation of the kinematic wave theory in traffic networks," in *Proc. 10th EWGT Meeting*, 2005, pp. 122–127.
- [22] M. P. H. Raadsen and M. C. J. Bliemer, "Continuous-time general link transmission model with simplified fanning, part II: Event-based algorithm for networks," *Transp. Res. B, Methodol.*, vol. 126, pp. 471–501, Aug. 2019. [Online]. Available: http://www.sciencedirect.com/science/article/pii/S0191261517301492
- [23] C. G. Claudel and A. M. Bayen, "Lax-Hopf based incorporation of internal boundary conditions into Hamilton-Jacobi equation. Part I: Theory," *IEEE Trans. Autom. Control*, vol. 55, no. 5, pp. 1142–1157, May 2010.
- [24] C. G. Claudel and A. M. Bayen, "Lax-Hopf based incorporation of internal boundary conditions into Hamilton-Jacobi equation. Part II: Computational methods," *IEEE Trans. Autom. Control*, vol. 55, no. 5, pp. 1158–1174, May 2010.
- [25] S. Osher and J. A. Sethian, "Fronts propagating with curvature-dependent speed: Algorithms based on Hamilton-Jacobi formulations," J. Comput. Phys., vol. 79, no. 1, pp. 12–49, Nov. 1988.
- [26] I. M. Mitchell, A. M. Bayen, and C. J. Tomlin, "A time-dependent Hamilton-Jacobi formulation of reachable sets for continuous dynamic games," *IEEE Trans. Autom. Control*, vol. 50, no. 7, pp. 947–957, Jul. 2005.
- [27] Y. T. Chow, W. Li, S. Osher, and W. Yin, "Algorithm for Hamilton–Jacobi equations in density space via a generalized hopf formula," *J. Sci. Comput.*, vol. 80, no. 2, pp. 1195–1239, Aug. 2019.
- [28] C. F. Daganzo, "On the variational theory of traffic flow: Well-posedness, duality and applications," *Netw. Heterogeneous Media*, vol. 1, no. 4, pp. 601–619, 2006.
- [29] J. A. Laval, G. Costeseque, and B. Chilukuri, "The impact of source terms in the variational representation of traffic flow," *Transp. Res. B. Methodol.*, vol. 94, pp. 204–216, Dec. 2016.
- [30] L. Leclercq, "Bounded acceleration close to fixed and moving bottlenecks," *Transp. Res. B, Methodol.*, vol. 41, no. 3, pp. 309–319, Mar. 2007. [Online]. Available: http://www.sciencedirect.com/science/article/pii/S0191261506000725
- [31] K. Moskowitz, "Discussion of 'freeway level of service as influenced by volume and capacity characteristics' by DR Drew and CJ Keese," *Highway Res. Rec.*, vol. 99, pp. 43–44, Jan. 1965.
- [32] G. F. Newell, "A simplified theory of kinematic waves in highway traffic," *Transp. Res. B*, vol. 27B, no. 4, pp. 281–303, 1993.
- [33] J.-P. Aubin, A. M. Bayen, and P. Saint-Pierre, "Dirichlet problems for some Hamilton–Jacobi equations with inequality constraints," SIAM J. Control Optim., vol. 47, no. 5, pp. 2348–2380, 2008.

- [34] Y. T. Chow, J. Darbon, S. Osher, and W. Yin, "Algorithm for overcoming the curse of dimensionality for time-dependent non-convex Hamilton–Jacobi equations arising from optimal control and differential games problems," *J. Sci. Comput.*, vol. 73, nos. 2–3, pp. 617–643, Dec. 2017.
 [35] J. Zhou, "Delay optimal control and viscosity solutions to associ-
- [35] J. Zhou, "Delay optimal control and viscosity solutions to associated Hamilton–Jacobi-Bellman equations," *Int. J. Control*, vol. 92, pp. 2263–2273, 2019.
- [36] M. Bardi and L. C. Evans, "On Hopf's formulas for solutions of Hamilton-Jacobi equations," *Nonlinear Anal., Theory, Methods Appl.*, vol. 8, no. 11, pp. 1373–1381, Jan. 1984.
- [37] J.-P. Aubin, "Viability solutions to structured Hamilton–Jacobi equations under constraints," SIAM J. Control Optim., vol. 49, no. 5, pp. 1881–1915, Jan. 2011.
- [38] G. De Nunzio, G. Gomes, C. C. de Wit, R. Horowitz, and P. Moulin, "Arterial bandwidth maximization via signal offsets and variable speed limits control," in *Proc. 54th IEEE Conf. Decis. Control (CDC)*, Dec. 2015, pp. 5142–5148.
- [39] C. G. Claudel and A. M. Bayen, "Solutions to switched Hamilton-Jacobi equations and conservation laws using hybrid components," in *Proc. 11th Int. Conf. Hybrid Syst. Comput. Control, Hybrid Syst., Comput. Control* in Lecture Notes in Computer Science, St. Louis, MO, USA, vol. 4981, M. Egerstedt and B. Mishra, Eds. Berlin, Germany: Springer, Apr. 2008, pp. 101–115.
- [40] J.-P. Aubin, Viability Theory (Systems and Control: Foundations and Applications). Boston, MA, USA: Birkhäuser, 1991.
- [41] J.-P. Aubin, "Viability kernels and capture basins of sets under differential inclusions," SIAM J. Control Optim., vol. 40, no. 3, pp. 853–881, Jan. 2001.
- [42] P. Cardaliaguet, M. Quincampoix, and P. Saint-Pierre, "Optimal times for constrained nonlinear control problems without local controllability," *Appl. Math. Optim.*, vol. 36, no. 1, pp. 21–42, Jul. 1997.
- [43] P. Saint-Pierre, "Approximation of the viability kernel," *Appl. Math. Optim.*, vol. 29, no. 2, pp. 187–209, Mar. 1994.
- [44] G. F. Newell, "A simplified theory of kinematic waves in highway traffic, part I: General theory," *Transp. Res. Part B: Methodol.*, vol. 27, no. 4, pp. 281–287, Aug. 1993.
- [45] A. M. Bayen, C. Claudel, and P. Saint-Pierre, "Computation of solutions to the Moskowitz Hamilton-Jacobi-Bellman equation under viability constraints," in *Proc. 46th IEEE Conf. Decis. Control*, 2007, pp. 4737–4742.
- [46] J. R. Taylor, Classical Mechanics. New York, NY, USA: Stony Brook University Science Books, 2005.
- [47] A. N. Sissakian, I. L. Solovtsov, and O. Y. Shevchenko, "Convergent series in variational perturbation theory," *Phys. Lett. B*, vol. 297, nos. 3–4, pp. 305–308, Dec. 1992. [Online]. Available: http://www.sciencedirect.com/science/article/pii/037026939291267D
- [48] A. Ambrosetti and P. H. Rabinowitz, "Dual variational methods in critical point theory and applications," *J. Funct. Anal.*, vol. 14, no. 4, pp. 349–381, Dec. 1973. [Online]. Available: http://www.sciencedirect.com/science/article/pii/0022123673900517
- [49] J. P. Lebacque, The Godunov Scheme and What it Means for First Order Traffic Flow Models. Amsterdam, The Netherlands: Elsevier, 1996.
- [50] S. K. Godunov, "A difference scheme for numerical solution of discontinuous solution of hydrodynamic equations," *Mat. Sbornik*, vol. 47, no. 3, pp. 271–306, 1959.
- [51] P.-E. Mazaré, A. H. Dehwah, C. G. Claudel, and A. M. Bayen, "Analytical and grid-free solutions to the Lighthill-Whitham— Richards traffic flow model," *Transp. Res. B, Methodol.*, vol. 45, no. 10, pp. 1727–1748, 2011. [Online]. Available: http://www.sciencedirect.com/science/article/pii/S0191261511001044



Yang Shao received the B.S. degree, the M.S. degree, and the Ph.D. degree in transportation engineering from Chang'an University, Xi'an, Shaanxi, China, in 2012, 2014, and 2019, respectively.

He is currently a Lecturer with the Xi'an University of Architecture and Technology, Xi'an. His research focuses on interchange design, traffic safety, and traffic flow.

Dr. Shao received a scholarship from the China Scholarship Council to study at The University of Texas at Austin as a Visiting Scholar.



Michael W. Levin received the B.S. degree in computer science and the Ph.D. degree in civil engineering from The University of Texas at Austin, Austin, TX, USA, in 2013 and 2017, respectively.

He is currently an Assistant Professor with the Department of Civil, Environmental, and Geo-Engineering, University of Minnesota, Minneapolis, MN, USA. His research focuses on traffic flow and network modeling of connected autonomous vehicles and intelligent transportation systems.

Dr. Levin was a recipient of the Dwight D. Eisenhower Fellowship from the Federal Highway Administration and the 2016 Milton Pikarsky Award from the Council of University Transportation



Christian G. Claudel received the Ph.D. degree in electrical engineering and computer science from the University of California at Berkeley (UC Berkeley), Berkeley, CA, USA, in 2010, and the M.S. degree in plasma physics from the Ecole Normale Superieure de Lyon, Lyon, France, in 2004.

He is currently an Assistant Professor of civil, architectural and environmental engineering with The University of Texas at Austin, Austin, TX, USA. His research interests include control and estimation of distributed parameter systems, wireless sensor

networks, and unmanned air vehicles.

Dr. Claudel received the Leon Chua Award from UC Berkeley in 2010 for his work on mobile millennium.



Stephen D. Boyles received the B.S. degrees in mathematics and civil engineering from the University of Washington, Seattle, WA, USA, in 2004, and the M.S. and Ph.D. degrees in civil engineering from The University of Texas at Austin, Austin, TX, USA, in 2006 and 2009, respectively.

He is currently an Associate Professor with the Department of Civil, Architectural, and Environmental Engineering, The University of Texas at Austin. His research projects span a broad array of topics, including static and dynamic traffic assignment, net-

work models for urban parking, multiscale network modeling, and planning for innovative vehicle technologies such as electric or autonomous vehicles.

Dr. Boyles received the 2015 New Faculty Award from the Council of University Transportation Centers, the 2015 Fred Burggraf Award of the Transportation Research Board, and the National Science Foundation Faculty Early Career Development (CAREER) Award.